

THE MECHANISM OF ELECTROPOLISHING OF NIOBIUM FROM CHOLINE CHLORIDE-BASED DEEP EUTECTIC SOLVENTS *

Qingwei Chu†, Andong Wu, Shichun Huang, Zhiming You, Hao Guo
Institute of Modern Physics, Chinese Academy of Sciences, Lanzhou, P. R. China

Abstract

The mechanism of electropolishing of niobium (Nb) from choline chloride-based deep eutectic solvent (DES) was studied by anodic polarization tests and electrochemical impedance spectroscopy (EIS) using a Nb rotating disk electrode (RDE). Based on the results of an anodic polarisation test, the electropolishing of Nb is mass transport controlled. EIS results are consistent with the compact salt film mechanism for niobium electropolishing in this electrolyte. The influence of rotation rate, applied potential and electrolyte temperature on the electropolishing mechanism of Nb was investigated. As the applied potential positively shift, R_{ct} , R_p and L increase, CPE decrease and R_s unchanged. The increase in rotation rate and electrolyte temperature leads to a decrease of R_s , R_{ct} , R_p and L , and an increase of CPE.

INTRODUCTIONS

The inner surface state of niobium cavity is thought to be one of the crucial factors in determining the performance of SRF cavity (unloaded quality factor and the maximum accelerating field). In recent years, electropolishing (EP) and buffered chemical polishing (BCP) are gradually becoming the chief means for SRF cavity treatments processes to eliminate the unevenness of the material's surface and to achieve possibly the highest surface smoothening effect. During the standard EP process, the electrolyte used for cleaning Nb surface is composed of HF and H₂SO₄ in a volume ratio of 1:9. BCP solution is an acid mixture of H₄PO₃, HF and HNO₃ by volume ratio of 1:1:1 or 2:1:1. EP and BCP have been widely used to remove the damaged layer and provide a superior surface finish, but BCP treatment normally produces an enhanced etching rate at grain boundaries and defect locations leading to a relatively rough Nb surface comparing with EP. However, these processes are not ideal due to the risk of personnel safety and the performance inconsistency of SRF cavities. The mixed acid solution has huge potential hazards for operating personnel and environment. Differ from other acids, HF can readily penetrate the skin, resulting in destruction of deep tissues layer, including bones. If HF is not rapidly neutralized and F- bound, tissues destruction may continue for days and often results in limb loss or death. Due to the hazard of HF, HF-free electrolyte for the electropolishing of Nb is an important research direction. As an alternative, some non-aqueous solvents, for example, ionic liquid, provide an alternative to replace hazardous acidic mixtures to try to overcome some drawbacks of the conventional EP and BCP mentioned above.

Ionic liquids have been utilised for a long time due to its particular features such as wide potential windows, thermal stability, high solubility of metal salts, high electrical conductivity, environmental safety and the opportunity for repeated usage. Abbott and co-workers introduced a relatively new class of ionic liquid, deep eutectic solvent (DES), based on eutectic mixtures of choline chloride (ChCl) with a hydrogen bond donor species [1]. DES, in particular, offers relatively low cost and low environmental impact. Some researchers have used DES for a range of metal finishing processes, including electropolishing of steel, Ni, Cu, Al and some biomedical alloys. However, to date, there are few studies on the electropolishing of Nb from DES. Tarek M. Abdel-Fattah et al. [2] used VB4 ionic liquid to smooth Nb samples. The authors believed that ionic liquid was a viable replacement for acid-based methods for preparation of SRF cavities. V. Pastushenko et al. [3] used Choline Chloride with Urea and different additives to polish Nb samples and cavities. It was found that mirror-like surfaces could be obtained at temperature higher than 120 °C, with high throwing power. However, the electropolishing mechanism of Nb from ionic liquid is unknown. It is critical to make clear of electropolishing mechanism for the optimization of electrolyte formulation and of operating parameters.

Nb was electropolished from a 1:2 ChCl-based ionic liquid in the present study. The aim of this work is to understand the electropolishing mechanism of Nb in more details by anodic polarization studies and electrochemical impedance spectroscopy (EIS) using a Nb RDE.

EXPERIMENTAL DETAILS

Choline chloride (ChCl) [HOC₂H₄N(CH₃)₃Cl, AR, ≥99.0%], urea [CON₂H₄, AR, ≥99.0%] and ammonium fluoride (AF) [NH₄F, AR, ≥99.0%] were used as obtained. The ChCl-based ionic liquid was formed by stirring the mixture of the two components in a mol ratio of 1ChCl: 2urea in a beaker at 80 °C until a homogeneous, colorless liquid formed. Then NH₄F was added to the mixture with gentle stirring to give a final ratio of 1ChCl: 2urea: 1AF.

Anodic polarization test and electrochemical impedance spectroscopy (EIS) were performed through an autolab PGSTAT302N electrochemical workstation with a three-electrode system. A pure Nb wire of 2 mm diameter was used as a RDE (working electrode). The wire was inserted into a Teflon holder exposing only the cross section as disc with a surface area of 0.0314 cm². An Al plate (10 mm×10 mm) was used as the counter electrode (CE) and an Ag/AgCl electrode as reference electrode (RE). Before each set of experiment, the electrodes were cleaned in an ultrasonic acetone bath, rinsed with distilled water and dried. The anodic polarisation curve of Nb RDE was

* Work supported by National Natural Science Foundation (11705252).

† email address: chuqingwei@impcas.ac.cn

measured by scanning a potential range from -1 V to 9.0 V (vs. Ag/AgCl) with a scan rate of 0.1 V/s. Electrochemical impedance spectroscopy (EIS) measurements were carried out by scanning a frequency range from 50 kHz to 1 Hz.

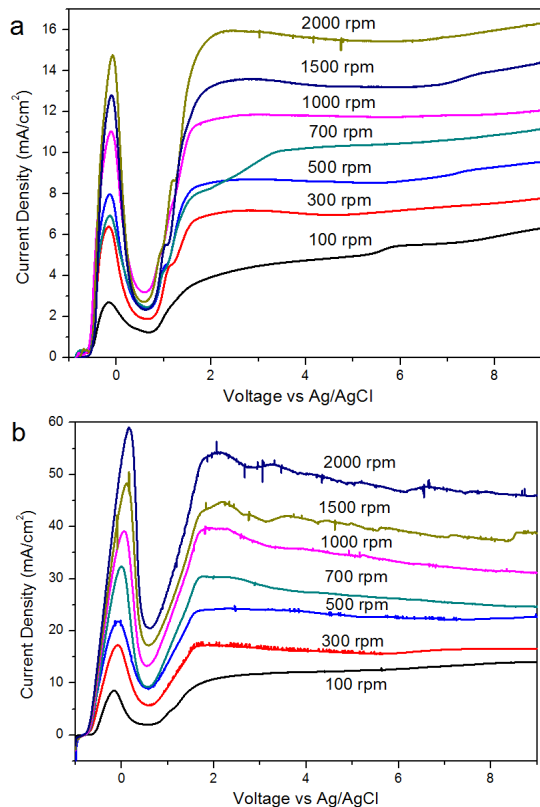


Figure 1: Anodic polarization curves of Nb RDE in DES at various rotation rates at temperatures of 60 oC (a) and 80 oC (b).

RESULTS AND DISCUSSION

Anodic polarization tests of Nb RDE were used to investigate electrode reaction kinetics of electropolishing in ChCl-based DES in a range of rotation rate (100 - 2000 rpm) at different temperatures (Fig. 1). A well-defined and wide potential range of limiting current density plateau (ranging from 3 V to 9 V) is exhibited in all the polarization curves. In this plateau range the current density is insensitive to the applied voltage which suggests a mass transport limited dissolution. The limiting current density increases with an increase in rotation rates, which is in accordance with a diffusion-controlled mechanism. High rotation rates can thin the thickness of the diffusion layer on Nb RDE surface and shorter the diffusion path length.

Compared with low temperature, the limiting current density is higher and less well defined with increasing electrolyte temperature (Fig.1b). The temperature effect is explained by the diffusion coefficient of dissolving species in the electropolishing bath, see Eq. (1)

$$D = D_0 \exp(-E_a/RT) \quad (1)$$

Where D_0 is the exponential pre-factor, E_a is the activation energy, R 8.314 J mol⁻¹ K⁻¹ is the gas constant and T is the

absolute temperature. The diffusion limiting current density can be described as Eq. (2)

$$i_L = nFD_0C\delta^{-1} \quad (2)$$

where n is the number of electrons transferred, F is Faraday constant, D is diffusion coefficient of dissolving species, C is the concentration of the electroactive species, δ is the thickness of the anodic diffusion layer. Combining Eq.(1) and (2):

$$i_L = nFD_0C\delta^{-1} \exp(-E_a/RT) \quad (3)$$

Following Eq.(3), increase of the temperature can result in an increase of the current density.

The Levich equation can reveal the diffusion and solution flow conditions around an RDE. Following the Levich behaviour conditions at RDE, the limiting current density can be calculated using Eq. (4)

$$i_L = 0.62nFD^{2/3}\nu^{-1/6}\omega^{1/2}C \quad (4)$$

where ν is kinematic viscosity, ω is the electrode rotation rate.

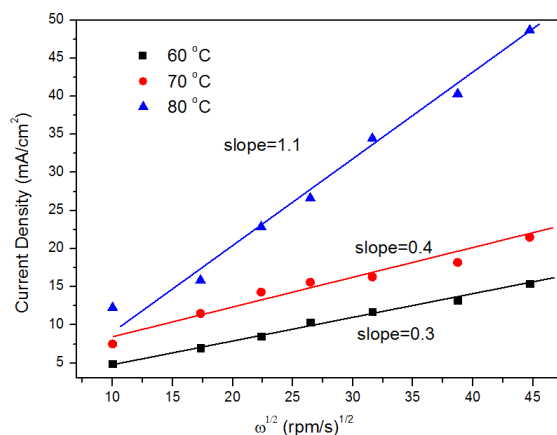


Figure 2: The limiting current density of Nb disk electrode plotted as a function of the square root of rotation rates.

The limiting current density taken from the current plateau at a potential of 5 V is plotted as a function of the square root of RDE rotation rates. The limiting current density approximately linearly increases and nonzero intercept with increase in $\omega^{1/2}$ at all temperatures studied as shown in Fig. 2. The linearly change follows Levich equation indicating a mass transport controlled process. The nonzero intercept may be due to the presence of electrode kinetic mechanism. The slope of curves dramatically increases with electrolyte temperature.

The relationships between current density and process temperature can be described by Arrhenius plot (Eq. 5-6) (see Ref. [4]).

$$i_L = k_0 \exp(-E_a/RT) \omega^{1/2} \quad (5)$$

$$\ln i_L = -E_a/RT + \ln(k_0\omega^{1/2}) \quad (6)$$

with constant and independent of temperature k_0 , gas constant R 8.314 J mol⁻¹ K⁻¹ and activation energy E_a . Figure 3 shows Arrhenius plot of the limiting current density as a function of the inverse of temperature with different rotation rates. The activation energy of the process deducing from the slope of the curves was approximate 48.5 kJ mol⁻¹.

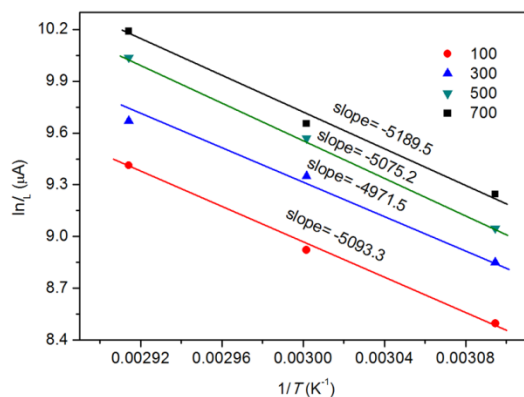


Figure 3: Arrhenius plot of the limiting current density at different rotation rate and temperature.

In order to investigate the mechanism of electropolishing, a series of EIS measurements was made at different electropolishing conditions namely, changing applied potential, rotation rate and electrolyte temperature (Figs. 4-6). Nyquist plots were measured at the applied potential 3-9 V at 70 °C within the limiting current plateau. The similar EIS curves have been also obtained at 50 °C, 60 °C and 80 °C. From Fig. 4, the diameter of the high-frequency semicircle arc increases with increasing applied potential. Additionally it is not a perfect semicircle in the high frequency regime which may be due to the non-uniform current-distribution effects on the surface of Nb RDE. The high frequency limit on the left intercept to the real axis represents the ohmic resistance (R_o) from reference to dissolving metal electrodes which is relatively insensitive to potential. In Fig. 5, the curves reveal that the diameter of the high-frequency semicircle decreases with increasing in rotation speed while there is almost no change on the left intercept (R_o). It is accorded with a salt film model that increasing rotation rate enhances ion transport in the electrolyte leading to thinner films and faster films dissolution rate [5]. The effect of temperature is reported in Fig. 6. A decrease in electrolyte temperature leads to an increase in diameter of the high-frequency loop due to decreasing electrolyte conductivity. All the Nyquist plots show a high frequency capacitive loop and a low frequency inductive loop. These results will be discussed in the next section.

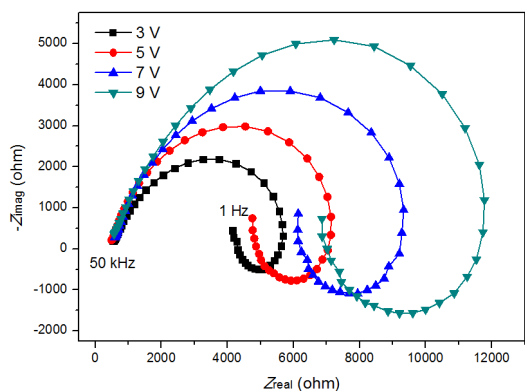


Figure 4: Nyquist plot of Nb RDE obtained at 3-9 V in stationary ionic liquid at 70 °C.

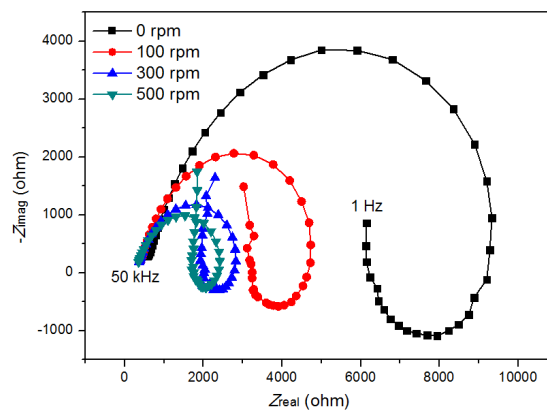


Figure 5: Nyquist plot of Nb RDE obtained at 7 V in ionic liquid at 70 °C. The rotation rate was 0, 100, 300 and 500 rpm.

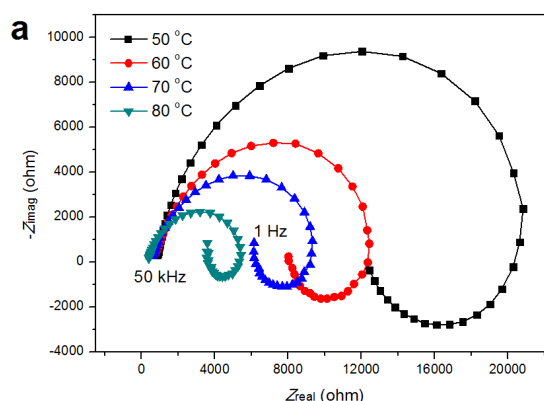


Figure 6: Nyquist plot of Nb RDE obtained at 7 V at different temperature. The rotation rate was 0 rpm.

It is critical to make clear of mass transport mechanisms in electropolishing systems for the optimization of electrolyte formulation and of operating parameters. Different mechanisms of electropolishing namely, the duplex salt-film model which has a duplex structure composed of an inner compact layer and an outer porous layer, and an adsorbate-acceptor model which looks at the role of adsorbed metallic species and the transport of the acceptor which solubilises them can be observed in the impedance spectra [6]. The existence of a salt film can be indicated by any of the following three responses: (i) the solution resistance R_s , varies with applied potential or rotation speed; (ii) the interface capacitance C_{dl} , changes with applied potential or rotation speed and (iii) the polarization resistance R_p , varies with applied potential [7].

The electrical circuit of the impedance makes deep analysis of Nyquist plot given in Fig. 7, in which a constant phase element $CPE(Q)$ connects in parallel with charge transfer resistance R_{ct} and inductance resistance RL , and RL connects in series with the inductor L . An ideal double-layer capacitance C_{dl} is replaced by $CPE(Q)$, and then the EIS results of the practical electrodes can be fitted more agreeably. By fitting impedance curves (Figs. 4-6), the values for variation of the impedance parameters as a function of the applied voltage, rotation rate and temperature can be obtained and are presented in

Content from this work may be used under the terms of the CC BY 3.0 licence (© 2019). Any distribution of this work must maintain attribution to the author(s), title of the work, publisher, and DOI.

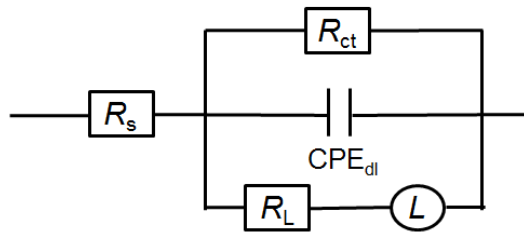


Figure 7: Equivalent circuit model for the impedance data.

Tables 1-3, respectively. The measured solution resistance R_s is roughly unchanged, independent of the applied potential, and R_s decreases as rotation rate and temperature increase. It is noticed that with the applied potential shift negatively, and rotation rate and temperature increase, the charge transition resistance R_{ct} decreases, which indicates the increase in the kinetics of the charge transfer reaction at the metal/oxide film interface and the capacitance of the film used to calculate the thickness of film decreases which conforms to the compact salt film model [8]. The high frequency capacitive loop is associated with a charge

transfer process and may be attributed to the presence of a protective salt film covering the surface of niobium. The low frequency inductive loop may be related to the relaxation process obtained by adsorption and incorporation of F^- ions on and into the salt film. With the potential decreases, and the rotation rate and temperature increase, the soluble products are more easily removed and increased mass transport furnishes larger quantities of F^- ion to the electrode surface which can lead to the decrease of L and R_L .

When an inductive loop is present, the polarization resistance R_p can be calculated from,

$$R_p = (R_L \times R_{ct}) / (R_L + R_{ct})$$

The polarization resistance R_p increases with the applied potential. The phenomenon indicates that a layer on the electrode surface thickens to compensate the potential drop along the limiting current plateau [5]. With increasing rotation rate and electrolyte temperature, R_p decrease. All the observations can suggest the existence of a compact salt film.

Table 1: Numerical Results for the Impedence Parameters as a Function of Applied Potential, from the Curves in Fig. 4

E (V) VS Ag/AgCl	R_s ($\Omega \cdot \text{cm}^2$)	R_{ct} ($\Omega \cdot \text{cm}^2$)	R_L ($\Omega \cdot \text{cm}^2$)	CPE-T ($\text{Sn.ohm}^{-1}/\text{cm}^2$)	CPE-P	L ($\text{H} \cdot \text{cm}^2$)	R_p ($\Omega \cdot \text{cm}^2$)
3	15.6	194.8	343.2	16.7×10^{-6}	0.77	3.9	124.3
5	14.2	239.6	373.8	7.2×10^{-6}	0.81	4.6	146.0
7	16.4	317.2	463.9	6.1×10^{-6}	0.81	5.9	188.4
9	14.6	418.4	471.4	6.1×10^{-6}	0.78	6.9	221.7

Table 2: Numerical Results for the Impedence Parameters as a Function of Rotation Speed, from the Curves in Fig. 5

Rotation Speed (rpm/s)	R_s ($\Omega \cdot \text{cm}^2$)	R_{ct} ($\Omega \cdot \text{cm}^2$)	R_L ($\Omega \cdot \text{cm}^2$)	CPE-T ($\text{Sn.ohm}^{-1}/\text{cm}^2$)	CPE-P	L ($\text{H} \cdot \text{cm}^2$)	R_p ($\Omega \cdot \text{cm}^2$)
0	16.4	317.2	463.9	6.1×10^{-6}	0.81	5.9	188.4
100	11.2	161.2	229.4	5.0×10^{-6}	0.83	0.62	94.7
300	9.1	99.8	144.9	8.2×10^{-6}	0.80	0.14	59.1
500	7.7	98.3	116.9	15.0×10^{-6}	0.74	0.067	53.4

Table 3: Numerical Results for the Impedence Parameters as a Function of Electrolyte Temperature, from the curves in Fig. 6

Temp. ($^{\circ}\text{C}$)	R_s ($\Omega \cdot \text{cm}^2$)	R_{ct} ($\Omega \cdot \text{cm}^2$)	R_L ($\Omega \cdot \text{cm}^2$)	CPE-T ($\text{Sn.ohm}^{-1}/\text{cm}^2$)	CPE-P	L ($\text{H} \cdot \text{cm}^2$)	R_p ($\Omega \cdot \text{cm}^2$)
50	27.4	690.4	914.3	3.3×10^{-6}	0.87	19.9	393.3
60	20.3	429.8	579.1	5.9×10^{-6}	0.81	7.3	246.7
70	16.4	317.2	463.9	6.1×10^{-6}	0.81	5.9	188.4
80	11.4	176.4	273.5	6.2×10^{-6}	0.84	1.7	107.2

CONCLUSIONS

In the present study, the electropolishing behavior of Nb from ChCl-based ionic liquid was examined. From the results obtained the following conclusions can be drawn.

- 1) The electropolishing of Nb is diffusion limited mass transport controlled.
- 2) EIS results are consistent with the compact salt film mechanism.
- 3) EIS quantitative study using RDE allowed to identify the effect of electropolishing parameters. As the applied potential positively shift, R_{ct} , R_p and L increase, CPE decrease and R_s unchanged. The increase in rotation rate and electrolyte temperature leads to a decrease of R_s , R_{ct} , R_p and L , and an increase of CPE.

REFERENCES

- [1] A.P. Abbott, D. Boothby, G. Capper, D.L. Davies, R.K. Rasheed, Deep Eutectic Solvents Formed between Choline Chloride and Carboxylic Acids: Versatile Alternatives to Ionic Liquids, *J. Am. Chem. Soc.* 126 (2004) 9142-9147.
- [2] A.I. Wixtrom, J.E. Buhler, C.E. Reece, T.M. Abdel-Fattah, Electrochemical Polishing Applications and EIS of a Novel Choline Chloride-based Ionic Liquid, in: W.M. Reichert, R.A. Mantz, P.C. Trulove, A. Ispas, D.M. Fox, M. Mizuhata, H.C. DeLong, A. Bund (Eds.) *Molten Salts and Ionic Liquids 18*, Honolulu, HI 2012, pp. 199-202.
- [3] V. B. Pastushenko, O. V. Malkova, V. Palmieri, A. A. Rossi, F. Stivanello, and G. Yu, "Fluorine Free Ionic Liquid Electropolishing of Niobium Cavities", in Proc. SRF'13, Paris, France, Sep. 2013, paper TUIOC03, pp. 410-413.
- [4] L. Neelakantan, A. Pareek, A.W. Hassel, Electro-dissolution of 30Nb-Ti alloys in methanolic sulfuric acid—Optimal conditions for electropolishing, *Electrochim. Acta* 56 (2011) 6678-6682.
- [5] K. Fushimi, L. Neelakantan, G. Eggeler, A.W. Hassel, On the Electropolishing Mechanism of Nickel Titanium in Methanolic Sulfuric acid – An Electrochemical Impedance Study, *Phys. Status Solidi A* 215 (2018) 1800011.
- [6] M. Matlosz, Modeling of impedance mechanisms in electropolishing, *Electrochim. Acta* 40 (1995) 393-401.
- [7] O. Piotrowski, C. Madore, D. Landolt, Electropolishing of tantalum in sulfuric acid-methanol electrolytes, *Electrochim. Acta* 44 (1999) 3389-3399.
- [8] H. Tian, S.G. Corcoran, C.E. Reece, M.J. Kelley, The Mechanism of Electropolishing of Niobium in Hydrofluoric-Sulfuric Acid Electrolyte, *J. Electrochem. Soc.* 155 (2008) D563.